27th EPS Conference on Contr. Fusion and Plasma Phys. Budapest, 12-16 June 2000 ECA Vol. **24B** *(2000) 1525 -1528*

Nonlinear MHD Effects in Fishbones

A. Ödblom, B.N. Breizman[1], S.E. Sharapov, T.C. Hender, and V.P. Pastukhov[2]

EURATOM/UKAEA Fusion Association, Abingdon, Oxfordshire OX14 3DB, UK.
[1]*Institute for Fusion Studies, UT, Austin, Texas 78712, USA.*
[2]*Russian Research Center "Kurchatov Institute", Moscow, Russia.*

1 Introduction

The global $n = 1$, $m = 1$ fishbone instability, driven by energetic ions, has been observed in nearly all tokamaks (see [1] and Refs. therein). Two different regimes have been discussed for the linear stage of this instability [2, 3]. The first regime refers to the case when the mode frequency ω is much greater than the bulk ion diamagnetic frequency ω_*. In this case, trapped energetic ions destabilise a continuum Alfvén mode that resonates with their precessional motion [2]. The instability develops when the kinetic ion drive exceeds the damping associated with the Alfvén resonances near the $q = 1$ surface. There are two resonance layers, one inside and one outside the q=1 surface. Their radial locations, r_A, are determined by $\omega^2 = (1 - q(r_A))^2 \times (V_A(r_A)/\ Rq(r_A))^2$, where $V_A(r)$ is the Alfvén velocity. Near the instability threshold, the width of each layer is a factor γ/ω smaller than the distance between the layers, where $\gamma << \omega$ is the instability growth rate.

The second regime refers to the fishbones with $\omega \approx \omega_*$ [3]. Continuum damping is negligible in this case since the mode lays within a frequency "gap" in the Alfvén continuum. As a result, the instability threshold is very low.

The characteristic burst-like structure of the fishbone oscillations and the significant decrease of the oscillation frequency of the mode within a single burst indicate that fishbones have a strongly nonlinear character [1]. There are two nonlinear effects particularly relevant to fishbones: (1) fluid nonlinearity of the background plasma near the $q = 1$ layer, and (2) kinetic nonlinearity of the fast particles, i.e. re-distribution of energetic ions in the phase space. The kinetic nonlinearity appears to be the dominant one when the fishbones are in the diamagnetic ω_* gap. The gap essentially eliminates the fluid resonance. This regime allows a perturbative description of the mode, which makes the problem technically similar to the bump-on-tail problem, as well as to many other wave-particle interaction problems [4]. The fishbones of the first type ($\omega >> \omega_*$) present a more challenging problem: an interplay of kinetic and fluid resonances. Linear responses from these resonances are almost equal near the instability threshold. However, their nonlinear responses are very different. In particular, one would expect the fluid nonlinearity to become important when the plasma displacement is comparable to the width of the resonant layer near the $q = 1$ surface, whereas the particle nonlinearity can still be negligible at this level.

In this work, we address the role of fluid nonlinearity for the $\omega >> \omega_*$ fishbones in the framework of an ideal reduced MHD model [5] combined with a linear response from the energetic particles. We demonstrate that the instability does not saturate during the nonlinear evolution before and while the two MHD resonant layers are merging near the $q = 1$ surface.

2 Reduced MHD model

We introduce two stream functions, $\dot{u}$ and α, to represent the components of the velocity and magnetic field perpendicular to the vacuum toroidal magnetic field $\mathbf{B}_T$:

$$\mathbf{V} = [\nabla \dot{u} \times \mathbf{B}_T], \qquad \mathbf{B} = \mathbf{B}_T + [\nabla \alpha \times \mathbf{B}_T]. \tag{1}$$

The ideal reduced MHD equations [5] were extended to include the pressure of trapped hot ions, $P_\perp$, that drives the instability, as follows

$$\dot{\alpha} = (\mathbf{B} \cdot \nabla)\dot{u}, \tag{2}$$

$$\Delta_\perp \ddot{u} = -(\mathbf{V} \cdot \nabla)\Delta_\perp \dot{u} + \frac{1}{4\pi\rho_0}(\mathbf{B} \cdot \nabla)\Delta_\perp \alpha - \frac{1}{\rho_0}\left[\mathbf{b}_T \times (\mathbf{b}_T \cdot \nabla)\mathbf{b}_T\right] \cdot \nabla \frac{P_\perp}{B_T}, \tag{3}$$

where $\boldsymbol{b}_T \equiv \boldsymbol{B}_T / |\boldsymbol{B}_T|$, and ρ_0 is the mass density of plasma. We consider an equilibrium with monotonic $q(r)$-profile and $q(0)<1$. The energetic ion pressure is localised close to the plasma centre, well inside the $q = 1$ surface (such as would be the case for alpha-particles). In the limit of a weak nonlinearity we consider a nonlinear interaction between three harmonics of the fishbone perturbation as follows:

$$u = u_1 e^{i\varsigma - i\vartheta - i\omega_0 t} + u_0 + u_2 e^{2[i\varsigma - i\vartheta - i\omega_0 t]} + c.c., \tag{4}$$

$$\alpha = \alpha_1 e^{i\varsigma - i\vartheta - i\omega_0 t} + (\alpha_0 + \tilde{\alpha}_0) + \alpha_2 e^{2[i\varsigma - i\vartheta - i\omega_0 t]} + c.c., \tag{5}$$

where α_0, $\tilde{\alpha}_0$ are the components of the stream functions representing the equilibrium poloidal magnetic field, and the nonlinearly generated poloidal magnetic field, respectively. ω_0 is the angular frequency of the perturbation near the linear threshold, $\omega_0 >> \gamma$. By substituting the values of $\tilde{\alpha}_0$, α_1 and α_2 from (2) in (3) and considering the layer regions, $r=r_A$, we obtain the following nonlinear MHD equations for the fishbone dynamics:

$$\ddot{\psi}_1' + \frac{V_A^2}{R^2}\left(1 - \frac{1}{q}\right)^2 \psi_1' = \rho(t)e^{-i\omega_0 t} - 2\frac{V_A^2}{R^2}\left(1 - \frac{1}{q}\right)^2 \psi_1'(\psi_1\psi_{-1})'' - 2\omega_0 \psi_1' \dot{\psi}_0', \tag{6}$$

$$\ddot{\psi}_0 = i\left[\omega_0^2 - \frac{V_A^2}{R^2}\left(1 - \frac{1}{q}\right)^2\right] \cdot (\psi_1 \psi_{-1}' - \psi_{-1}\psi_1'), \tag{7}$$

where $\psi_1 \equiv -B_T u_1 / r$, $\psi_0 \equiv B_T \tilde{u}_0 / r$. The contribution from the second harmonic to our problem is found to be much smaller than the retained nonlinear terms. We took into account that the perturbed pressure of the hot ions, $\delta P_\perp$, enters the equation in the form of an integral over the radius:

$$\frac{1}{r_*^3}\int_0^{r_*} r^2 \left\{\frac{1}{\rho_0}\left[\mathbf{b}_T \times (\mathbf{b}_T \cdot \nabla)\mathbf{b}_T\right] \cdot \nabla \frac{\delta P_\perp}{B_T}\right\}_1 dr = \frac{\rho(t)}{B_T} e^{-i\omega_0 t}, \tag{8}$$

where $q(r_*) = 1$ and the closure equation that relates $\delta P_\perp$ and $\psi_1(-\infty)$ is obtained by integrating the linearised drift kinetic equation for the hot ions. As long as the fast particle response is linear, the quantity $\rho(t)$ is a linear functional of $\psi_1(-\infty;t)$. In this work, we use a model relation between $\rho(t)$ and $\psi_1(-\infty;t)$ in the form

$$\rho(t)\exp(-i\omega_0 t) \equiv -\frac{\Omega'}{\pi} K \int_{-\infty}^{t} \frac{T\dot{\psi}_1(-\infty;\tau)d\tau}{[T - i(\tau - t)]^2}, \qquad \Omega \equiv \frac{V_A}{R}\left(1 - \frac{1}{q}\right) \tag{9}$$

where T is a characteristic precession period for fast particles, $\Omega' = d\Omega / dr$, and the dimensionless parameter K is a normalized energetic particle content.

3 Analysis

The model for the energetic particle response (9) leads to the following linear dispersion relation:

$$\mathrm{i} = K\int_0^\infty \frac{z\exp(-z)}{z-\omega T - i0}\mathrm{d}z, \tag{10}$$

from which we find that the threshold value of K for the instability is $K_0 \cong 0.91$, and that the mode frequency at the threshold is $\omega_0 \cong 1.35/T$. We then solve (6), (7) iteratively assuming that $K - K_0 << K_0$. The linear solution $\psi_1^{(0)}$ reads

$$\psi_1^{(0)} = \int_\infty^x dx_1 \int_0^\infty d\tau \frac{\sin\Omega\tau}{\Omega}\rho(t-\tau)e^{-i\omega_0(t-\tau)}, \tag{11}$$

and the solution of the next order gives a cubic nonlinear equation for the mode amplitude a, $\psi_1(-\infty;\mathrm{t}) \equiv a\exp(-\mathrm{i}\omega_0\mathrm{t})$, which can be presented in the following normalized form:

$$\exp(i\phi)\frac{da}{dt} = a - i\int_0^\infty d\tau\int_0^\infty d\tau_1\int_0^{t-\tau} d\tau_2(\tau+\tau_1)a(t-\tau-\tau_1)$$
$$\times\left[a^*(\tau_2-\tau-\tau_1)a(\tau_2) - a^*(\tau_2-\tau-\tau_1)a(\tau_2)\right]. \tag{12}$$

Here, the phase ϕ is determined by the near threshold expression that gives $\tan\phi = 0.38$. The solution of (12) grows explosively and becomes singular at a finite time t_0:

$$a = \frac{R}{(t_0-t)^2}\exp[i\sigma\ln(t_0-t)], \tag{13}$$

Here, R and σ are constants determined by the governing equation

$$ie^{i\phi} = R^2\int_0^\infty dx\int_0^x dz\frac{ze^{i\sigma\ln\left(\frac{(1+x)(1+z)}{1+x+z}\right)}}{(1+x)^2(1+z)^2(1+x+z)^2}\left\{\frac{2+i\sigma}{2-i\sigma}\frac{z+x}{1+z+x} - \frac{z}{1+x} - \frac{x}{1+z}\right\}. \tag{14}$$

The σ dependence of the phase of the double integral on the RHS of (14) is shown in Fig. 1. For $\tan\phi = 0.38$ we note that the phase of the double integral should be -1.21 which from graphical inspection in Fig. 1 gives the solution to (14) for σ as $\sigma \cong -6.5$, i.e. a down chirp in frequency.

No saturation due to the MHD nonlinearity exists for the fishbone on the early phase of the instability. However, at a later stage of the instability, when the two Alfvén resonance layers $r=r_A$ merge and form a single broad layer at the $q = 1$ surface, a nonlinear saturation mechanism similar to [6] should dominate the nonlinear MHD evolution. Numerical analysis is however required for the study of the nonlinear effects at this stage.

4 Numerical Results

The reduced MHD equations (2) and (3), including a linear model for the perturbation of the fast particle pressure, have been analysed numerically based on an initial value spectral code in cylindrical geometry.

When the energetic particle pressure is close to the instability threshold $\beta_{h,crit} \sim sr\omega/V_A$, the top-hat linear eigenmode profile splits up into a two step structure around the $q = 1$ surface due to the finite frequency of the mode, $\Delta \sim rR\omega/sV_A$ (s denotes the magnetic shear). The numerical solution is in quantitative agreement with the linear analytical eigenmode profile as illustrated in Fig. 2 where $\gamma/\omega \cong 8\%$. Also, the simulations agree with analytical predictions for the mode frequency and the growth rate near the instability threshold. The mode growth accelerates nonlinearly as shown in Fig. 3, which is in agreement with analytical expectations, and is accompanied with frequency chirping. From Fig. 3 we note that the accelerated growth is well described by only the m=n=0 and the m=n=1 harmonics. The double layer structure is lost in the nonlinear phase when γ~ω as examplified in Fig. 4, and there is no indication of a slowing down of the growth rate before or while the layers merge.

Acknowledgements Drs Hender and Sharapov were funded jointly by EURATOM and the UK Department of Trade and Industry. Dr Ödblom was funded by a Marie Curie grant. Dr Breizman was supported by U.S. DOE Contract No. DE-FG03-96ER-54346.

[1] W W Heidbrink and G Sadler, Nuclear Fusion **34**, 535 (1994)
[2] L Chen, R B White and M N Rosenbluth, Phys. Rev. Lett. **52**, 1122 (1984)
[3] B Coppi and F Porcelli, Phys. Rev. Lett. **57**, 2272 (1986)
[4] R B White, Theory of tokamak plasmas, Amsterdam (1989)
[5] H R Strauss, Phys. Fluids **19**, 134 (1976)
[6] M N Rosenbluth, R Y Dagazian and P H Rutherford, Phys. Fluids **16**, 1894 (1973)

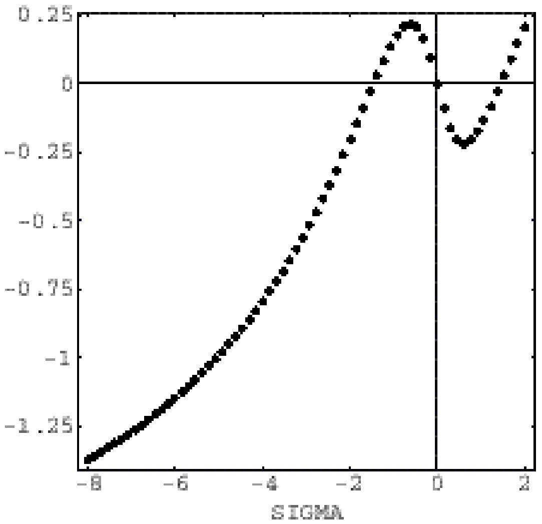

Fig. 1. The argument of the double integral in Eq. (14) as a function of σ.

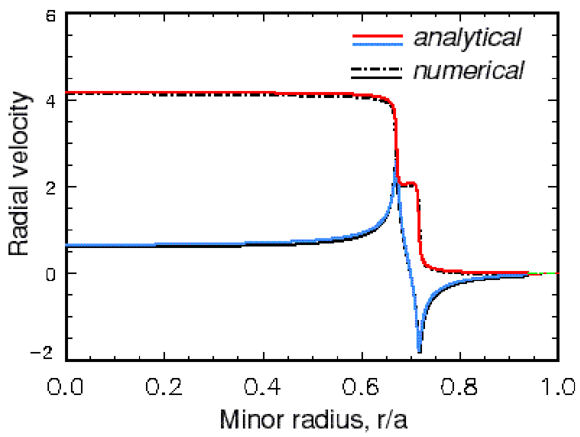

Fig. 2. The real and imaginary part of the n=m=1 Fourier component of the linear radial velocity profile [arbitrary units].

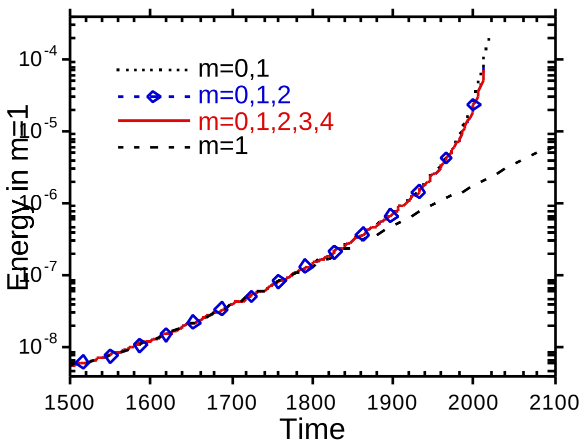

Fig. 3. The time evolution of the total energy content in the m=n=1 harmonic for various number of angular harmonics [arbitrary units].

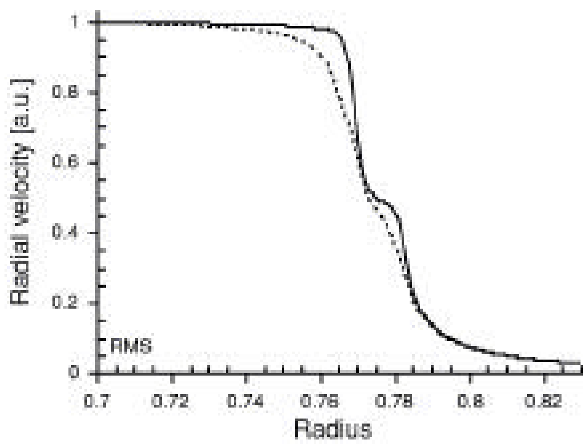

Fig. 4. The radial velocity profile in the linear (solid) and nonlinear (dashed) regime.